Journal of Archaeological Science (2003) **30,** 429–438
doi:10.1006/jasc.2002.0852

Discriminating Proboscidean Taxa Using Features of the Schreger Pattern in Tusk Dentin

Josh Trapani and Daniel C. Fisher

Museum of Paleontology and Department of Geological Sciences, University of Michigan, 1109 Geddes Road, Ann Arbor, MI 48109-1079, U.S.A. jtrapani@umich.edu; dcfisher@umich.edu

(*Received 15 January 2002, revised manuscript accepted 10 May 2002*)

The Schreger pattern is a characteristic structural feature of proboscidean tusk dentin. We document features of the Schreger pattern in mastodons, mammoths, and Asian and African elephants. Discriminant function analyses of Schreger pattern features are highly successful in distinguishing mastodons from mammoths (>95%), mammoths from extant elephants (>99%), and small samples of extant elephant taxa from each other (100%). Schreger pattern features vary with location on a tusk; however, even when tusk location information is excluded or unknown, discriminant function analyses of Schreger pattern features successfully assign single samples to the correct taxon in 73–93% of cases. Even on small fragments or worked artifacts, measurements of Schreger pattern may be made in more than one location on the specimen; these additional measurements enhance the discriminatory power of the pattern. To maximize discriminatory power, we recommend assessing fragments or artifacts for clues to location on the tusk and making measurements in multiple locations. The ability of the Schreger pattern to distinguish tusk dentin of proboscidean taxa should prove useful to archaeologists in a variety of contexts.

Keywords: ELEPHANTS, PROBOSCIDEANS, TUSKS, IVORY, SCHREGER PATTERN, DENTIN.

Introduction

The mammalian order Proboscidea includes the extant Asian (*Elephas maximus*) and African (*Loxodonta africana* and *L. cyclotis*) elephants, as well as their fossil relatives. Human–proboscidean interactions have occurred in a variety of contexts throughout human history and in geographically widespread locations. Whether directly or indirectly, these interactions have often involved proboscidean tusks (enlarged, ever-growing incisors) or "ivory" (proboscidean tusk dentin). Despite the importance of ivory in human history and technology, it remains a poorly understood substance. In this study, we investigate features of the Schreger pattern in proboscidean tusk dentin and demonstrate the utility of the pattern in aiding archaeologists and others in discriminating tusks, tusk fragments, and worked ivory artifacts from various proboscidean taxa.

The Schreger pattern, also sometimes referred to as an "engine-turning" or "checkerboard" pattern, was first described by Bernard Schreger (1800), see also Espinoza & Mann (1993). It is unique to proboscidean dentin, and best developed in tusks (though also present in premolars and molars of some taxa). The Schreger pattern is so characteristic of proboscidean tusk dentin that Richard Owen (1845) defined "ivory" by its presence. The Schreger pattern should not be confused with the better-known "Hunter-Schreger bands" (sometimes referred to as "bands of Schreger" in older literature) present in mammalian enamel.

In a transverse section of tusk, the Schreger pattern consists of sets of intersecting "lines" radiating in spiral fashion from the tusk axis (Figure 1). Light and dark regions forming these lines are thought to be macroscopic manifestations of systematic shifts in undulatory pathways of dentinal tubules, produced by odontoblasts as they move towards the tusk axis during dentin deposition (Miles & White, 1960; Miles & Boyde, 1961; Miles & Poole, 1967; Figure 1). "Schreger lines" extend obliquely across adjacent tubules, following tracts in which the tubules show the same phase of undulation (Bradford, 1967; Boyde, 1968), and spiral dextrally or sinistrally around the tusk axis. The "Schreger angle" is the angle of intersection of dextral and sinistral Schreger lines. Many Schreger lines are not continuous throughout the radial thickness of the tusk. Total number of lines changes—often decreasing by deletion towards the tusk axis—a phenomenon that may be related to differential packing of odontoblasts and differences in dentinal tubule densities with varying distance from the tusk axis (Saunders, 1979; Raubenheimer *et al*., 1998; JT, pers. obs.).

The ability to distinguish tusks and tusk fragments of various proboscidean taxa from one another is

0305–4403/03/$-see front matter

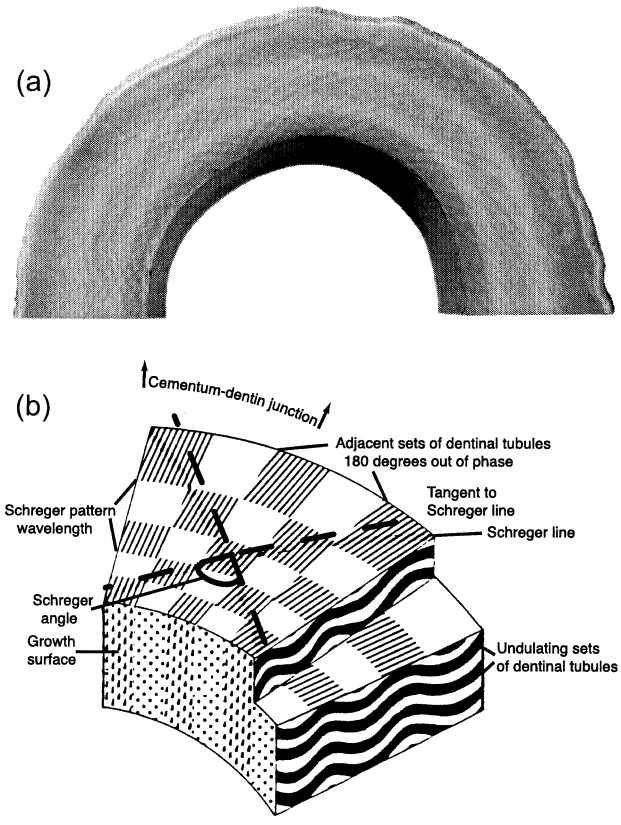

Figure 1. (a) Polished transverse section (perpendicular to tusk axis) of part of an *Elephas maximus* (UMMZ 157850) tusk, showing Schreger pattern; arcuate interior surface in shadow is part of the pulp cavity near the proximal end of the tusk; a thin cementum layer is present on outer surface of tusk (tusk diameter is 4 cm). (b) Schematic block diagram showing Schreger pattern features in transverse and radial section (modified from Miles & Poole, 1967). During dentin deposition, sets of odontoblasts move in phase with each other and 180° out of phase with adjacent sets, producing alternating light and dark areas that resemble a checkerboard. Schreger lines, angles, and wavelengths are described in the text. The growth surface is progressively displaced towards the tusk axis and away from the cementum-dentin junction (CDJ).

important in a variety of contexts. Identifying the species from which a given culturally associated ivory sample was derived may provide information on the procurement or trading practices of the people under study. For example, it is unknown whether *Loxodonta* or *Elephas* (or both) was the source of ivory used in Greece and the Aegean during the Late Bronze Age (Hayward, 1990). Likewise, ivory foreshafts (Dunbar, 1991) were crafted by late Pleistocene inhabitants of North America and there is great interest in determining which of the sympatric proboscidean taxa were used as sources of raw material (Herrera, 1999).

The ability to distinguish proboscidean tusks may also be useful in regulating contemporary hunting and trade in ivory. In 1989, importation of African elephant ivory was banned by international treaty (CITES: Convention on International Trade in Endangered Species) to help protect remaining elephant populations. However, ivory from woolly mammoth (*Mammuthus primigenius*) is legal to trade and makes up a substantial part of contemporary ivory traffic; some way to distinguish ivory of modern species and *Mammuthus* is necessary (Espinoza & Mann, 1994). Penniman (1952), though not addressing conservation questions, was the first to recognize a difference in the Schreger pattern between mammoths and elephants. He noted that mammoth Schreger lines were finer and closer together than elephant lines, producing smaller Schreger angles. He believed that these pattern differences were the result of the greater curvature of mammoth tusks.

Espinoza & Mann (1991, 1993) used Schreger pattern features, specifically Schreger angle values, to distinguish tusk dentin of elephants and mammoths. They found that "outer" Schreger angle values (from near the cementum-dentin junction, or CDJ) from African elephants are obtuse (mean = 124·15°; S.D., 13·35°), whereas "outer" values from woolly mammoths are acute (mean = 73·21°; S.D., 14·71°). This provides an easy, visual way of determining whether an ivory specimen is legal or illegal. Other workers interested in conservation and forensic questions have used trace element analysis (Prozesky *et al.*, 1995; Shimoyama *et al.*, 1998) and nondestructive Raman spectroscopy (Edwards & Farwell, 1995; Edwards *et al.*, 1997*a*, *b*, 1998; Shimoyama *et al.*, 1997) to distinguish tusks and artifacts of *Loxodonta*, *Elephas*, and *Mammuthus* from each other.

In addition to using Schreger angle values to distinguish African elephant from mammoth dentin, Espinoza & Mann (1993) measured "outer" angles on three mastodon and three gomphothere samples. They report these as falling within their reported mammoth range of 35°–115°. In contrast, Fisher *et al.* (1998) measured maximal (not restricted to the "outer" region near the CDJ) angle values on mastodon and mammoth tusks and found no overlap between the ranges of this variable for these two taxa; mastodon maximal values were greater.

Here we use a suite of features of the Schreger pattern (not just Schreger angle) and assess their power to discriminate between sets of proboscidean taxa. We attempt to discriminate mammoths from mastodons, "fossil" (*Mammuthus*) from "modern" (*Elephas* and *Loxodonta*) dentin, and finally we present preliminary data on discriminating the two extant proboscidean genera from one another.

Materials and Methods

Material used in this study is shown in Table 1. Specimens of extant proboscideans are Recent; mastodons (*Mammut americanum*) and mammoths (*Mammuthus columbi* and *M. primigenius*) are from the late Pleistocene of North America. Our mammoth sample includes two *Mammuthus primigenius*, a few

Table 1. Material examined in this study

Taxon	Specimen	Sex	Location	No. measurements
Elephas maximus	"Mini" (zoo animal—UMMZ 157850)	F		8
Loxodonta africana	"J51" (wild—UMMP)	M		11
Mammut americanum	Farview (RMSC)	M	New York	10
	Grandville (GRPM)	M	Michigan	21
	Miller (UMMP 11736)	F	Michigan	8
	Parker (AC)	M	Michigan	15
	Powers (WMU)	F	Michigan	26
Mammuthus primigenius	FMNH (P 25481)	F	Alaska	33
	FMNH (P 14175)	M	Alaska	20
Mammuthus sp.	Scarborough (MSM 90·69)	F	Maine	31
	Poyser (UMMP 10603)	M	Indiana	27
Mammuthus columbi	HSMS (5 individuals)	M	South Dakota	8
	Jensen (UNSM)	M	Nebraska	2

Abbreviations: AC=Alma College; FMNH=Field Museum of Natural History; GRPM=Grand Rapids Public Museum; HSMS=Hot Springs Mammoth Site; MSM=Maine State Museum; RMSC=Rochester Museum and Science Center; UMMP=University of Michigan Museum of Paleontology; UMMZ=University of Michigan Museum of Zoology; UNSM=University of Nebraska State Museum; WMU=Western Michigan University.

individuals of *M. columbi*, and two individuals currently unassignable to species. Our sample of extant proboscideans is small, but both mammoth and mastodon samples include multiple measurements from several individuals for which complete or nearly complete tusks were available. These individuals represent a wide geographic range and both sexes, thus providing a reasonable assessment of intraspecific variability.

Many of these tusks had already been sampled as part of an ongoing study of proboscidean life history (e.g., Fisher, 1996). In these cases, sampling for life history reconstruction began with a longitudinal cut down the entire length of the tusk, slightly off the tusk axis. A second, parallel cut produced a thin (approximately 1 cm) slab encompassing the entire tusk length and showing the "cone-within-cone" incremental structure of the dentin. Cuts were made into this slab at regular intervals along its length, producing blocks of dentin from which transverse thin sections were prepared, oriented perpendicular to incremental growth laminae and extending from the tusk axis to the CDJ. By choosing sample locations to ensure temporal overlap between successive samples, variations in increment thickness and isotopic composition can be traced along the entire tusk, providing a detailed picture of conditions during an animal's lifetime (e.g., Fisher, 1990, 1996, 2001). For incomplete tusks or tusks where longitudinal cuts were not feasible, samples were taken in as many locations as were accessible and practical. This sampling strategy, though not designed specifically for the current study, provided assessment of variability throughout tusks in addition to comparisons between taxa.

Data for each individual consisted of measurements taken at various radial distances along transects at several proximodistal locations. Data regarding location on the tusk recorded distances from the tusk tip and from the tusk axis. Distance from the tusk tip was measured to the nearest 10 mm. Distance from the tusk axis was referenced to annual incremental features. We assigned each increment a thickness and an "average" distance from the tusk axis, to the nearest 0·1 mm.

We assessed wavelength (the distance over which dentinal tubules move through one complete undulation; see Figure 1) within each annual increment by counting the number of light–dark cycles along the radial thickness of the increment at three to five places and taking an average. Within the thickness of dentin represented by each increment, we also measured a "representative" Schreger angle. Schreger angle was measured with a rotating stage placed under a stereomicroscope with crosshairs on one ocular. We centred the point on the tusk at which Schreger angle was to be assessed under the crosshairs, and measured the angle through which the stage had to be rotated to bring each of the two Schreger lines intersecting at that point successively into tangency with the same crosshair. We measured each angle three times and took the average. Total range of repeated measures of the same angle was usually 3° or less.

We also made an assessment of the pattern's qualitative appearance within a given increment based on the scheme in Figure 2, which illustrates the continuum of possible appearances. The presence or absence of each of the three pattern types (referred to as "V" or "X" based on resemblances to those letters or "C" for "checkerboard") were scored for each increment. Measuring angle, wavelength, and qualitative appearance of the pattern in one location allowed us to associate these variables with one another in a multivariate analysis.

We performed discriminant function analyses (see Albrecht, 1980 and Campbell & Atchley, 1981) using SPSS 9.0 Statistical Software. Taxon was used as the

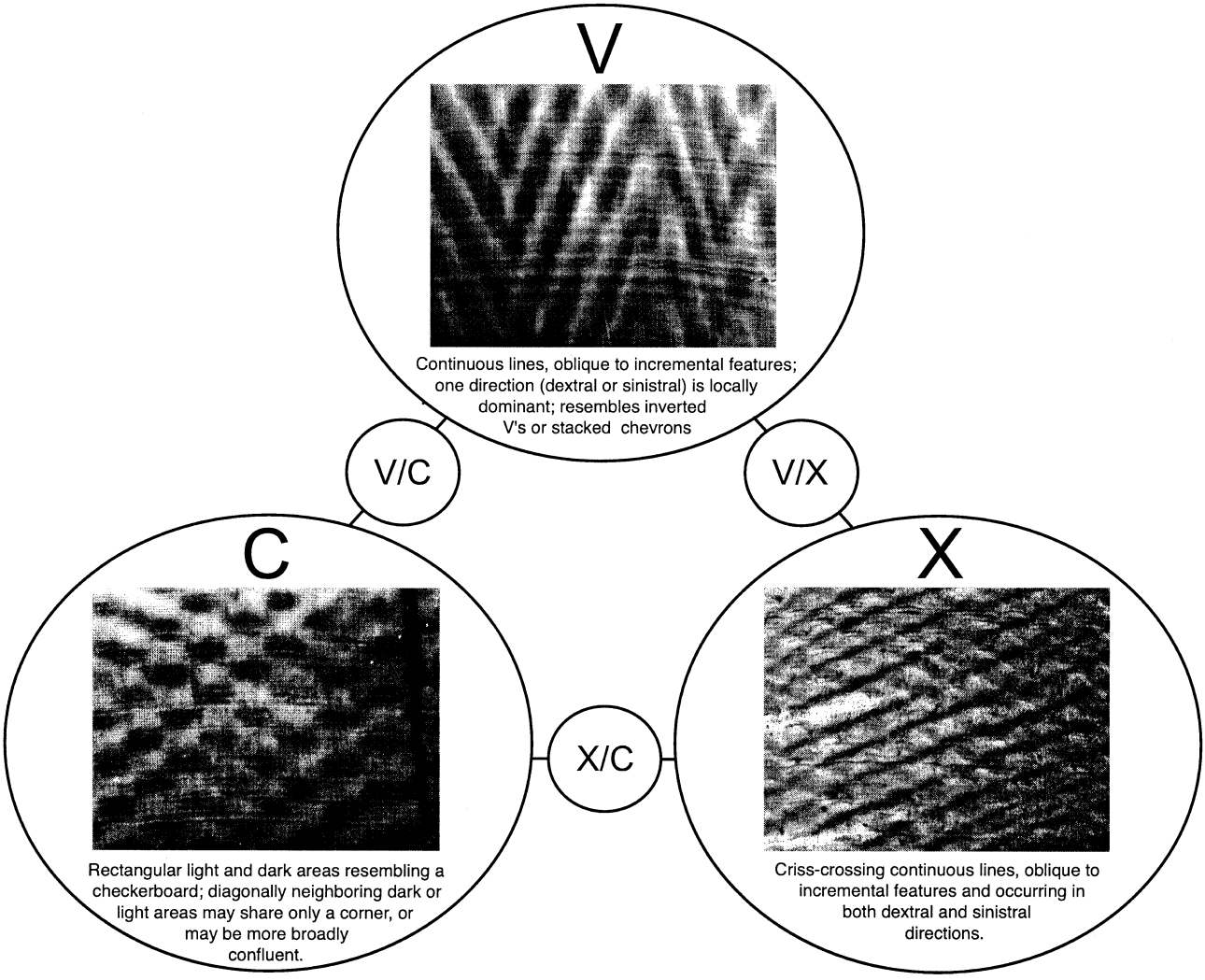

Figure 2. Categories of qualitative appearance used to classify the Schreger pattern. "V", "C", and "X" are end-members in a continuum of variation, within which "V/C", "V/X", and "X/C" indicate intermediate patterns or areas where both end-member patterns were present together. "V" and "X" are named because the corresponding patterns resemble these letters. "C" stands for "checkerboard". Each image is a transverse section perpendicular to the "growth surface"; width of each image is 0·9 cm and height is 0·68 cm. Fine, approximately horizontal, dark-light couplets are incremental features marking former positions of the surface of dentin apposition ("growth surface"). Dentin apposition proceeds from the CDJ towards the tusk axis (downwards in each frame). The "V" frame is from near the tusk axis on a mammoth, the "C" frame is from the region of maximum Schreger angle on a mastodon, and the "X" frame is also from a mastodon, closer to the CDJ.

grouping variable. Prior to analysis, measures on a linear scale (distances and average wavelength in mm) were logged ($\log_{10}$), and Schreger angle was arcsine-transformed (Zar, 1984) to equalize variances. Presence/absence of each pattern type were treated as binary variables. Each analysis was run twice: once with all variables included, and once with logged distances from tusk tip and tusk axis excluded, to assess how discriminatory power changed when spatial locations of samples on the tusk were unknown (as they would be for many tusk fragments and artifacts).

Results

Table 2 shows discriminant function coefficients for each of the analyses. The absolute value of each loading reflects the relative contribution of each variable to each discriminant function. In all three cases, distance from tusk axis and Schreger angle contribute most heavily to the discrimination of taxa. With tusk location data excluded, Schreger angle contributes most heavily to discrimination of taxa in all three cases. However, in the discrimination of *Elephas* and *Loxodonta*, both wavelength and presence/absence of the "V" pattern contribute nearly as heavily as Schreger angle.

Discriminating mastodons from mammoths

The classification matrix for the analyses attempting to discriminate *Mammuthus* and *Mammut* is shown in Table 3, and histograms of discriminant scores are

Table 2. Discriminant function coefficients for the discriminant function analyses performed in this study, with and without information on location on the tusk

Variable	*Mammuthus* vs. *Mammut*		"Modern" vs. "Fossil"		*Elephas* vs. *Loxodonta*	
	With location	Without location	With location	Without location	With location	Without location
Distance from tusk tip	−0·175		0·110		0·764	
Distance from tusk axis	0·952		−1·352		3·332	
Wavelength	0·341	0·368	−0·056	−0·027	0·658	0·974
Schreger angle	−1·302	−0·894	1·524	1·074	−2·313	1·064
"V" pattern	0·172	0·237	−0·065	0·111	1·022	0·948
"X" pattern	0·227	0·304	−0·286	−0·350	−0·247	−0·674
"C" pattern	0·111	0·138	0·167	0·328	−0·305	−0·181

shown in Figure 3. Discrimination with tusk location information included in the analysis is more accurate, but both with and without this information, discrimination of samples from these taxa is over 90% accurate.

Discriminating "fossil" from "modern" ivory

The purpose of these analyses was to determine how well extant proboscidean dentin could be distinguished from mammoth dentin specifically. "Fossil" thus refers to *Mammuthus* only, and "modern" to *Elephas* and *Loxodonta* grouped together. The classification matrix is shown in Table 4, and histograms of discriminant scores in Figure 4. Discrimination when tusk location information is included in the analysis is nearly perfect (>99%). Without such information, correct classification drops to about 85% of cases. It is worth adding, however, that in the context of stopping the importation of illegal ivory, *Loxodonta* is a much more important source of ivory than *Elephas*. A histogram broken down by taxon (Figure 4C) shows that most of the more extreme "modern" values in the "fossil" range represent *Elephas* samples.

Discriminating Elephas *from* Loxodonta

The classification matrix for these analyses is shown in Table 5, and histograms of discriminant scores in Figure 5. Sample sizes are small, but our data indicate that discrimination with tusk location information included is perfect. When such information is not included, discrimination is around 73–88% accurate.

Table 3. Classification matrix from the discriminant function analysis of Mammuthus *vs.* Mammut

	Mammuthus	*Mammut*	Total	% correct
With location				
Mammuthus	117	4	121	96·7
Mammut	3	77	80	96·3
Without location				
Mammuthus	110	11	121	90·9
Mammut	6	74	80	92·5

Our small sample suggests that *Loxodonta* is more likely to be mistaken for *Elephas* than vice versa.

Discussion

These results indicate that multivariate consideration of Schreger pattern features provides an effective tool for discriminating between tusk material of different proboscidean taxa. Further, while analyses in which tusk location information was included provided more powerful discrimination, even without this information, correct assignment of a sample to its taxon was possible in 73–93% of cases.

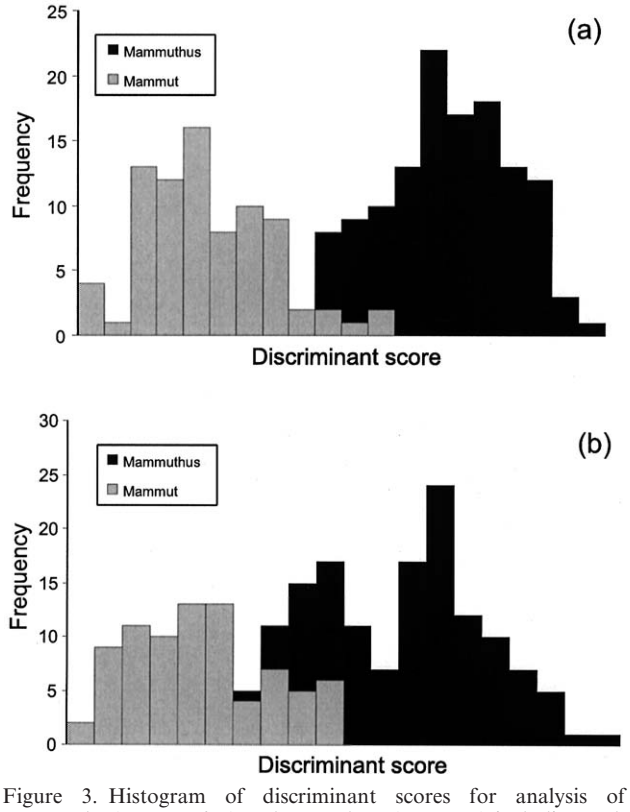

Figure 3. Histogram of discriminant scores for analysis of mammoths (*Mammuthus*) and mastodons (*Mammut*) including tusk location information (a) and excluding tusk location information (b).

Table 4. Classification matrix from the discriminant function analysis of "Modern" vs. "Fossil" dentin

	"Modern"	"Fossil"	Total	% correct
With location				
"Modern"	19	0	19	100·0
"Fossil"	1	120	121	99·2
Without location				
"Modern"	16	3	19	84·2
"Fossil"	17	104	121	86·0

In fact, the discriminant function analyses presented above may be considered conservative in their ability to assign samples to taxa because they attempt to make assignments based upon single sets of measures. On even the smallest tusk fragments or artifacts, multiple locations for measurement should be available. Measuring multiple sets of data on the same piece provides more powerful discrimination because pattern features vary in taxon-specific ways, as described in more detail below.

Combinations of pattern features are taxon-specific and may aid researchers in assigning tusk fragments or artifacts to a taxon even in cases where quantitative multivariate analysis is not possible. Mammoths reach maximum Schreger angle values of approximately 70°–100° near the CDJ; mastodons reach maximum values of approximately 100°–145° about halfway between axis and CDJ. Mammoths rarely show the "C" pattern common in mastodons, while mastodons lack the "V" pattern common near the tusk axis in mammoths. Mammoths typically have wavelengths of 1 mm or greater, and wavelength greatly increases at low Schreger angle and near the tusk axis. Mastodons have wavelengths of less than 1 mm, and wavelength remains essentially invariant with Schreger angle and distance from the axis.

These criteria highlight the importance of spatial (especially with respect to distance from the tusk axis) variation in pattern features. Proximodistal and radial location may affect the criteria useful for distinguishing tusks. Identification of tusk fragments and worked artifacts is therefore more challenging than identification of isolated, whole tusks, because the location on the tusk from which the fragment or artifact comes may not be known. When attempting to diagnose fragments and artifacts, it is useful to assess location on the tusk as accurately as possible. We recommend examining fragments/artifacts for clues to location, including the presence of cementum or the tusk axis within the fragment, and the radius of curvature of incremental features (features are more tightly curved near the axis).

Of course, many tusk fragments and artifacts will not present perfect transverse sections, and either oblique exposures or uncontrolled viewing angles may distort Schreger pattern features. However, this

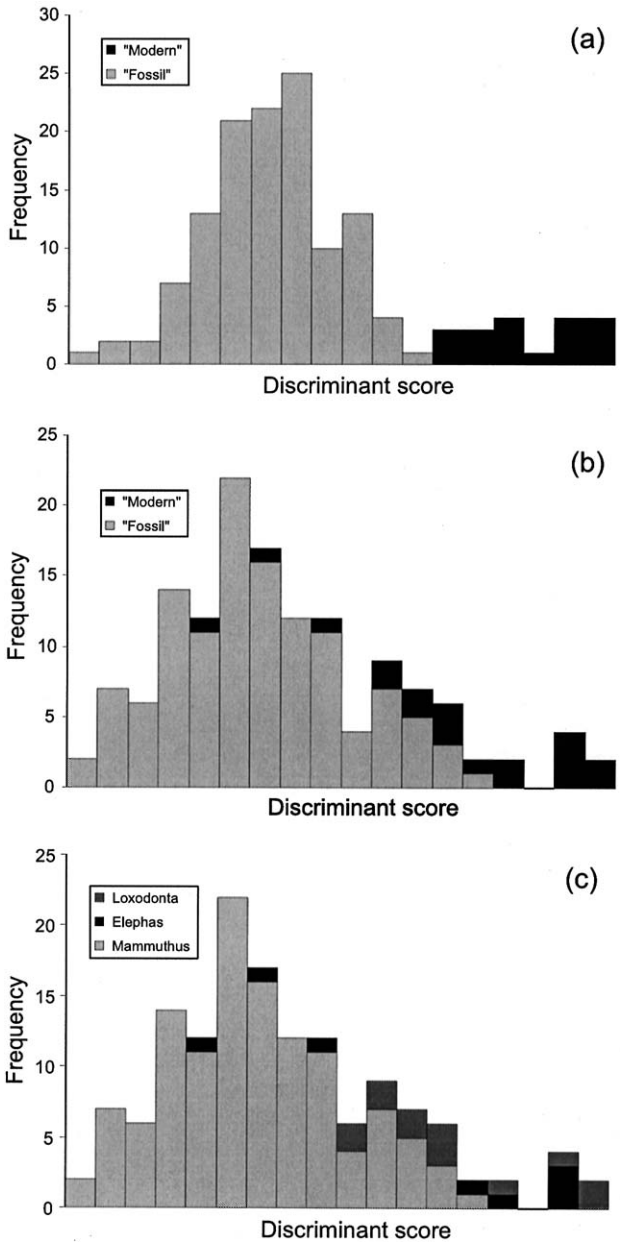

Figure 4. Histogram of discriminant scores for analysis of "fossil" ivory (i.e., mammoths) and "modern" ivory (*Elephas* and *Loxodonta*) including tusk location information (a), excluding tusk location information (b), and broken up to show differences in scores between the modern taxa (c).

tendency can be largely controlled by selecting an appropriate viewing direction—parallel to the tusk axis, which is a symmetry axis of the radially organized, three-dimensional system of structural elements of which tusk dentin is comprised. Although sectioning and polishing provide optimum conditions for viewing Schreger pattern features, they are not generally essential. Natural fractures and naturally (or artificially) abraded surfaces often follow the structural heterogeneities responsible for the Schreger pattern, allowing

Table 5. Classification matrix from the discriminant function analysis of Loxodonta *vs.* Elephas

	Loxodonta	*Elephas*	Total	% correct
With location				
Loxodonta	11	0	11	100·0
Elephas	0	8	8	100·0
Without location				
Loxodonta	8	3	11	72·7
Elephas	1	7	8	87·5

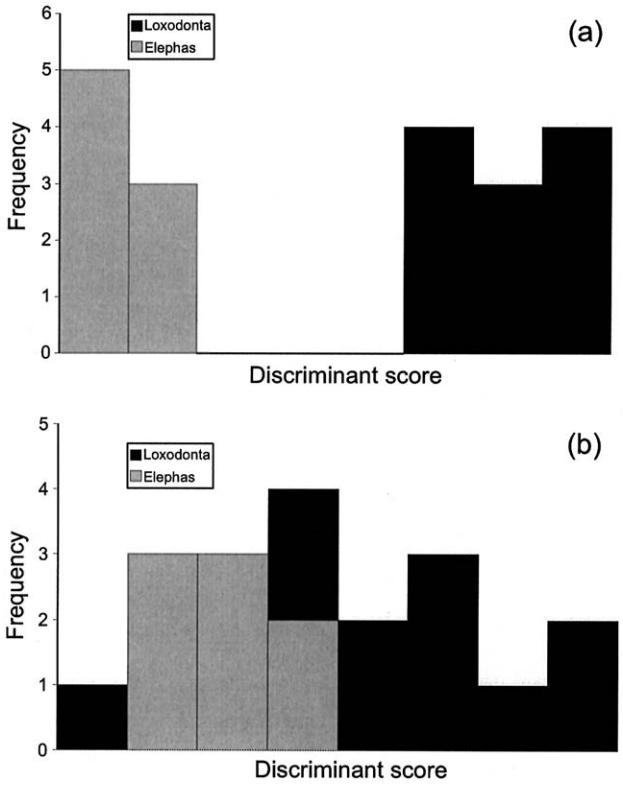

Figure 5. Histogram of discriminant scores for analysis of African (*Loxodonta*) and Asian (*Elephas*) elephants including tusk location information (a) and excluding tusk location information (b).

it to be observed (from topographic or textural cues) without alteration of original specimens. In addition, application of volatile, non-aqueous fluids such as kerosene or acetone may provide transient, reversible enhancement of Schreger pattern features due to differential absorption and alteration of physical properties (e.g., effective surface roughness and index of refraction). Again, combinations of pattern features, especially when assessed in multiple locations, may usually be interpreted readily.

Our samples show no clear evidence of sexual dimorphism in the Schreger pattern in taxa for which both sexes are present in our sample. It is possible that the Schreger pattern may be useful for looking at finer-scale taxonomic differences than those addressed here (e.g. differences between *Mammuthus primigenius* and *M. columbi*, or between *Loxodonta* species). At present, our sample is inadequate for tackling these questions. However, we have established clear differences at the generic level. In addition, a sample of Miocene *Gomphotherium* tusk dentin (a subset of the individuals used in the study by Fox, 2000) analysed in similar fashion is readily distinguished from most other proboscidean genera (see Figure 5A in Fox (2000) for an example of the Schreger pattern in *Gomphotherium*). There are other aspects of tusks such as size and morphology, growth increment features, and characteristic qualities of the dentin itself which may also be useful for discriminating proboscidean taxa; some of these are reviewed in Haynes (1991).

Discriminating mastodons from mammoths

Differences in location of Schreger angle measurement most likely account for the discrepancy in the findings of Espinoza & Mann (1993) and Fisher *et al.* (1998) with respect to mastodon and mammoth Schreger angle values. Espinoza and Mann (1993) measured angles near the CDJ. Fisher *et al.* (1998) measured maximum angles. We observed that mastodons reach maximum angle values of about 140° at around 50% to 70% of the distance to the CDJ, declining to values of about 100°–120° near the CDJ. Highest angle values occur within transects taken more than 400 mm away from the tusk tip. Mastodons show "X", "C", and intermediate patterns along the entire axis-to-CDJ radius, but most "C" patterns are concentrated near the highest angle values. Mastodon wavelengths remain relatively short (less than 1 mm) and roughly constant regardless of Schreger angle or distance from tusk axis.

In contrast, mammoths reach maximum angle values of around 100° near the CDJ. As in mastodons, highest angle values occur in transects taken more than 400 mm from the tusk tip. Mammoths show "X" and rarely "C" patterns near the CDJ; "V" patterns are more common at low angle values near the tusk axis. Mammoth wavelengths are relatively long (usually greater than 1 mm) and become very long at low Schreger angles and near the tusk axis, often associated with a transition from "X" to "V" patterns.

Discriminant function analyses correctly predict group membership of samples in over 95% of cases. Surprisingly, given the spatial variation in the pattern, group membership is correctly predicted in over 90% of cases even when tusk location information is excluded. This highlights the utility of Schreger pattern features in distinguishing these two taxa, even when location on the tusk is unknown.

The classification functions for this and the other analyses discussed in this paper are provided in the Appendix and may be used to assign new, unknown samples to taxon. The ability to use aspects of the

Schreger pattern to determine the taxonomic identity of tusk fragments and ivory artifacts should be useful to paleontologists interested in Pleistocene biogeography, as well as archaeologists interested in human–proboscidean interactions.

Discriminating "Modern" from "Fossil" ivory

Espinoza & Mann (1991, 1993) used "outer" Schreger angles to distinguish dentin of *Loxodonta* and *Mammuthus primigenius*. The salient features of mammoth dentin have been summarized above. Both *Loxodonta* and *Elephas* are distinguished from *Mammuthus* by possessing larger Schreger angles, and like mammoths, both possess their highest angle values near the CDJ. Angle values for *Elephas* are as high as 120°, and values for *Loxodonta* as high as 135°. The extant taxa also possess longer wavelength values than *Mammuthus*. *Elephas* lacks the "V" pattern common near the tusk axis in *Mammuthus*.

Discriminant function analyses indicate perfect discrimination of *Mammuthus* from modern taxa when tusk location information is known, and around 85% accuracy without this information. As with the analysis of mammoths and mastodons, measuring Schreger pattern features in more than one location on a specimen will enhance discriminating power.

Discriminating Elephas *from* Loxodonta

Discriminant scores show perfect discrimination between these taxa when tusk information is included (Figure 5A). However, we must qualify these results in view of the small sample sizes examined. We have only one specimen of each taxon, and only partial tusks. In particular, our Asian elephant specimen is female, possessing only a small tusk, and is thus an unlikely ivory source. In addition, we do not know whether our *Loxodonta* specimen is *L. africana* or *L. cyclotis* (Roca *et al*., 2001), and cannot comment on pattern differences between these species. Obtaining samples of extant taxa comparable to our sample of mastodons and mammoths (i.e., multiple complete tusks sectioned at a series of proximodistal locations) is difficult for a variety of legal and financial reasons. However, our results tentatively suggest that Schreger pattern features may discriminate these two taxa, which will be of interest to archaeologists attempting to source Old World ivories and apply this information to archaeological problems (e.g., Hayward, 1990). Confirmation of these results would require a larger sample including individuals of both sexes and more thorough assessment of proximodistal and intraspecific variation of Schreger pattern parameters.

Conclusions

The Schreger pattern is characteristic of the tusk dentin of most Pleistocene and Recent proboscideans, and provides a powerful tool for discriminating proboscidean taxa and answering a variety of archaeological questions. Past attempts to use aspects of the Schreger pattern (specifically Schreger angle) for discriminating taxa, though somewhat successful, are complicated by spatial variation in the pattern. We have shown that assessing multiple features of the pattern, especially at multiple locations on a single specimen, may help overcome this complication, even in cases where location on the tusk is unknown. We advise attempting to assess location on the tusk as well as possible, measuring multiple pattern features in multiple locations, and viewing pattern features in a direction parallel to the tusk axis (equivalent to projecting them onto a transverse plane).

Schreger pattern features easily distinguish tusk dentin of *Mammuthus primigenius* and *M. columbi* from *Mammut americanum*, and *Mammuthus* from *Loxodonta* and *Elephas maximus*. We have also presented preliminary data suggesting that Schreger pattern features may distinguish extant genera from one another. A larger sample and use of individuals of both sexes would be necessary to confirm this possibility.

Acknowledgements

We thank Scott Beld for preparing material, and David Fox for discussion and access to gomphothere material. Gerry Smith and Bill Sanders commented on drafts of the manuscript; Ken Guire, Gerry Smith, and Miriam Zelditch provided statistical discussion and advice. Bonnie Miljour aided with figure production. We also thank the numerous researchers who prompted us to write this paper by asking for advice on identifying their tusk fragments or artifacts. J.T. was funded by a University of Michigan Regents Fellowship and a National Science Foundation Graduate Fellowship during the course of this work. D.C.F. was funded by National Science Foundation Grant EAR-9628063.

References

Albrecht, G. H. (1980). Multivariate analysis and the study of form, with special reference to canonical variate analysis. *American Zoologist* **20,** 679–693.

Boyde, A. (1968). Comparative histology of mammalian teeth. In (A. A. Dahlberg, Ed.) *Dental Morphology and Evolution*. Chicago: University of Chicago Press, pp. 81–94.

Bradford, E. W. (1967). Microanatomy and histochemistry of dentine. In (A. E. W. Miles, Ed.) *Structural and Chemical Organization of Teeth, Volume II*. New York: Academic Press, pp. 3–33.

Campbell, N. A. & Atchley, W. R. (1981). The geometry of canonical variates analysis. *Systematic Zoology* **30,** 268–280.

Dunbar, J. S. (1991). Resource orientation of Clovis and Suwanee Age Paleoindian sites in Florida. In (R. Bonnichsen & K. L. Turnmire, Eds) *Clovis Origins and Adaptations*. Corvallis: Center for the Study of the First Americans, pp. 185–213.

Edwards, H. G. M. & Farwell, D. W. (1995). Ivory and simulated ivory artefacts: Fourier transform Raman diagnostic study. *Spectrochimica Acta Part A* **51,** 2073–2081.

Edwards, H. G. M., Farwell, D. W., Holder, J. M. & Lawson, E. E. (1997*a*). Fourier-transform Raman spectroscopy of ivory: II. Spectroscopic analysis and assignments. *Journal of Molecular Structure* **435,** 49–58.

Edwards, H. G. M., Farwell, D. W., Holder, J. M. & Lawson, E. E. (1997*b*). Fourier-transform Raman spectroscopy of ivory: III. Identification of mammalian specimens. *Spectrochimica Acta Part A* **53,** 2403–2409.

Edwards, H. G. M., Farwell, D. W., Holder, J. M. & Lawson, E. E. (1998). Fourier transform Raman spectroscopy of ivory: a non-destructive diagnostic technique. *Studies in Conservation* **43,** 9–16.

Espinoza, E. O. & Mann, M. J. (1991). *Identification guide for ivory and ivory substitutes*. Baltimore: World Wildlife Fund and Conservation Foundation.

Espinoza, E. O. & Mann, M. J. (1993). The history and significance of the Schreger pattern in proboscidean ivory characterization. *Journal of the American Institute for Conservation* **32,** 241–248.

Espinoza, E. O. & Mann, M. J. (1994). Mammoth or elephant ivory? Forensics provides the key. *Endangered Species Technical Bulletin* **19,** 8–9.

Fisher, D. C. (1990). Age, sex, and season of death of the Grandville mastodont. *The Michigan Archaeologist* **36,** 141–160.

Fisher, D. C. (1996). Extinction of proboscideans in North America. In (J. Shoshani & P. Tassy, Eds) *The Proboscidea*. Oxford: Oxford University Press, pp. 296–315.

Fisher, D. C. (2001). Season of death, growth rates, and life history of North American mammoths. In (D. L. West, Ed.) *Mammoth Site Studies*. Proceedings of the First International Conference on Mammoth Site Studies. *Publications in Anthropology* 22. Lawrence: University of Kansas, pp. 121–135.

Fisher, D. C., Trapani, J., Shoshani, J. & Woodford, M. (1998). The Schreger pattern in mastodon and mammoth tusk dentin. *Current Research in the Pleistocene* **15,** 105–107.

Fox, D. L. (2000). Growth increments in *Gomphotherium* tusks and implications for late Miocene climate change in North America. *Palaeogeography, Palaeoclimatology, Palaeoecology* **156,** 327–348.

Haynes, G. (1991). *Mammoths, Mastodonts, & Elephants: Biology, behavior, and the fossil record*. Cambridge: Cambridge University Press.

Hayward, L. G. (1990). The origin of the raw elephant ivory used in Greece and the Aegean during the Late Bronze Age. *Antiquity* **64,** 103–109.

Herrera, J. (1999). Determining the species source of prehistoric ivory. *Aucilla River Times* **12,** 17. http://www.flmnh.ufl.edu/natsci/vertpaleo/aucilla12_1/ivory99.htm.

Miles, A. E. W. & Boyde, A. (1961). Observations on the structure of elephant ivory. *Journal of Anatomy* **95,** 450 (abstract).

Miles, A. E. W. & Poole, D. F. G. (1967). The history and general organization of dentitions. In (A. E. W. Miles, Ed.) *Structural and Chemical Organization of Teeth, Volume I*. New York: Academic Press, pp. 3–43.

Miles, A. E. W. & White, J. W. (1960). Ivory. *Proceedings of the Royal Society of Medicine* **53,** 775–780.

Owen, R. (1845). *Odontography*. London: H. Bailliere.

Penniman, T. K. (1952). Pictures of ivory and other animal teeth, bone, and antler. *Pitt Rivers Museum Occasional Papers on Technology* **5,** 1–37.

Prozesky, V. M., Raubenheimer, E. J., Van Heerden, W. F. P., Grotepass, W. P., Przybylowicz, W. J., Pineda, C. A. & Swart, R. (1995). Trace element concentration and distribution in ivory. *Nuclear Instruments and Methods in Physics Research B* **104,** 638–644.

Raubenheimer, E. J., Bosman, M. C., Vorster, R. & Noffke, C. E. (1998). Histogenesis of the chequered pattern of ivory of the African elephant (*Loxodonta africana*). *Archives of Oral Biology* **43,** 969–977.

Roca, A. L., Georgiadis, N., Pecon-Slattery, J. & O'Brien, S. J. (2001). Genetic evidence for two species of elephant in Africa. *Science* **293,** 1473–1477.

Saunders, J. J. (1979). A close look at ivory. *The Living Museum* **41,** 56–59.

Schreger, B. N. G. (1800). Beitrag zur Geschichte der Zähne. *Beitrage für die Zergliederungkunst* **1,** 1–7.

Shimoyama, M., Maeda, H., Sato, H., Ninomiya, T. & Ozaki, Y. (1997). Nondestructive discrimination of biological materials by near-infrared Fourier transform Raman spectroscopy and chemometrics: discrimination among hard and soft ivories of African elephants and mammoth tusks and prediction of specific gravity of the ivories. *Applied Spectroscopy* **51,** 1154–1158.

Shimoyama, M., Nakanishi, T., Hamanaga, Y., Ninomiya, T. & Ozaki, Y. (1998). Non-destructive discrimination between elephant ivory products and mammoth tusk products by glancing incidence X-ray fluorescence spectroscopy. *Journal of Trace and Microprobe Techniques* **16,** 175–182.

Zar, J. H. (1984). *Biostatistical Analysis*. Englewood Cliffs: Prentice Hall.

Appendix

Classification functions derived in this study, with and without information on location on the tusk. To assign a new case to taxon, multiply the coefficients below by the measured value for each corresponding variable (transformed appropriately) and sum these weighted variables plus the constant. Assign each new case to the group for which the sum is greatest. For presence/absence of the "V", "X", and "C" patterns, we used "0" to indicate absence and "1" to indicate presence

	With location		Without location	
Variable	*Mammut*	*Mammuthus*	*Mammut*	*Mammuthus*
(A) Discriminating mammoths and mastodons				
Distance from tusk tip	20·79491	19·05270		
Distance from tusk axis	− 19·95148	− 7·77859		
Wavelength	− 13·57417	− 6·09230	− 4·08120	2·13157
Schreger angle	121·62263	78·06526	103·92563	80·96332
"V" pattern	17·39586	19·22572	18·03109	19·96265
"X" pattern	− 0·12754	1·73927	− 0·54457	1·37181
"C" pattern	− 1·73550	− 0·71481	− 2·56511	− 1·58815
Constant	− 72·12175	− 53·31306	− 47·05224	− 31·84018
	"Modern"	"Fossil"	"Modern"	"Fossil"
(B) Discriminating "modern" and "fossil" taxa				
Distance from tusk tip	15·32159	14·18599		
Distance from tusk axis	− 19·46566	2·92255		
Wavelength	30·82041	32·82901	41·74216	42·25002
Schreger angle	170·63359	116·24394	152·33826	132·46282
"V" pattern	19·90468	20·52223	20·92781	20·38169
"X" pattern	− 8·09913	− 5·59129	− 8·24260	− 6·65109
"C" pattern	2·25615	0·34998	1·26118	− 0·68218
Constant	− 78·13333	− 65·63571	− 61·73900	− 47·51864
	Elephas	*Loxodonta*	*Elephas*	*Loxodonta*
(C) Discriminating Asian and African elephants				
Distance from tusk tip	324·88646	374·89059		
Distance from tusk axis	64·61728	180·07669		
Wavelength	218·37483	252·96789	79·83780	90·36560
Schreger angle	125·52723	3·37587	126·40189	137·96128
"V" pattern	58·41496	80·36975	47·87172	52·05921
"X" pattern	− 10·48375	− 14·73358	12·72657	10·33936
"C" pattern	− 14·30933	− 18·46520	0·25595	− 0·25135
Constant	− 456·91181	− 606·96323	− 57·84260	− 65·19966